INSTITUTE OF PHYSICS PUBLISHING PLASMA PHYSICS AND CONTROLLED FUSION

Plasma Phys. Control. Fusion **48** (2006) 1501–1513 doi:10.1088/0741-3335/48/10/004

How much laser power can propagate through fusion plasma?

Pavel M Lushnikov[1,2,3] **and Harvey A Rose**[3,4]

[1] Landau Institute for Theoretical Physics, Kosygin St. 2, Moscow, 119334, Russia
[2] Department of Mathematics and Statistics, University of New Mexico, Albuquerque, NM 87131, USA
[3] Theoretical Division, Los Alamos National Laboratory, MS-B213, Los Alamos, New Mexico, 87545, USA

E-mail: har@lanl.gov

Received 17 March 2006, in final form 2 August 2006
Published 11 September 2006
Online at stacks.iop.org/PPCF/48/1501

Abstract

Propagation of intense laser beams is crucial for inertial confinement fusion, which requires precise beam control to achieve the compression and heating necessary to ignite the fusion reaction. The National Ignition Facility (NIF), where fusion will be attempted, is now under construction. Control of intense beam propagation may be ruined by laser beam self-focusing. We have identified the maximum laser beam power that can propagate through fusion plasma without significant self-focusing and have found excellent agreement with recent experimental data. This maximum is determined by the collective forward stimulated Brillouin scattering instability which suggests a way to increase the maximum power by appropriate choice of plasma composition with implication for NIF designs. Our theory also leads to the prediction of anti-correlation between beam spray and backscatter and therefore raises the possibility of indirect control of backscatter through manipulation of plasma ionization state or acoustic damping. We find a simple expression for laser intensity at onset of enhanced beam angular divergence (beam spray).

(Some figures in this article are in colour only in the electronic version)

1. Introduction

Propagation of intense laser beams in plasma raises outstanding technological and scientific issues. These issues are closely tied with inertial confinement fusion (ICF) [1–4] which requires precise beam control in order to maintain symmetry of spherical target implosion and

[4] Author to whom any correspondence should be addressed.

so achieve the compression and heating necessary to ignite the fusion reaction. ICF will be attempted at the National Ignition Facility (NIF). While most engineering features of NIF are now fixed, there are still crucial choices to be made [4] in target designs. Control of intense beam propagation is endangered by laser beam self-focusing, when a beam digs a cavity in plasma, trapping itself, leading to higher beam intensity, a deeper cavity and so on.

Self-focusing occurs when an intense laser beam propagates through a wide range of optical media [5] and has been the subject of research for more than 40 years, since the advent of lasers [6]. In laser fusion the intensity of laser beams is so large that self-focusing in plasma can cause disintegration of a laser beam into many small beams, leading to rapid change in beam angular divergence, $\Delta\theta$, called beam spray. Significant beam spray is absolutely unacceptable for attaining fusion which requires precise laser beam control [4]. It was commonly assumed that the main source of beam spray in fusion plasma is the self-focusing in local maxima of laser intensity (hot spots) which are randomly distributed throughout the plasma [4]. Hot spot self-focusing can be controlled by reducing beam correlation time, T_c. However we show in this paper that the main limitation of maximum beam power, which can propagate in plasma without significant beam spray, is determined by collective instability which couples the beam to an ion acoustic wave. We call this instability *collective* forward stimulated Brillouin scatter (CFSBS) [7] because it does not depend on the dynamics of isolated hot spots but rather the intensity fluctuations as temporally smoothed (averaged) by ion inertia. We show below that this collective instability is consistent with the first experimental observation of beam spray onset [8] while hot spot self-focusing is not. We find a simple expression for laser intensity at onset of enhanced beam angular divergence (beam spray), suitable for use in ICF design codes.

2. Beam collapse (catastrophic self-focusing)

There are two self-focusing mechanisms in plasma: ponderomotive and thermal. Historically, ponderomotive self-focusing was studied first. The ponderomotive mechanism results from averaging over fast electron oscillations in the laser electromagnetic field, at frequency ω_0. Averaging induces an effective electrostatic potential proportional to the local laser intensity, which in turn adds to the usual fluid pressure term in hydrodynamical equations [9]. The thermal mechanism results from Ohmic heating induced electron temperature fluctuations.

Ponderomotive self-focusing in three-dimensions (3D) is quite different than in two-dimensions (2D). (Here one dimension is the direction of propagation of laser beam with one/two transverse dimensions in 2D/3D, respectively.) In 2D, self-focusing often results in propagation of optical pulses (called solitons [10]) without change of their shape over large distances. In 3D, self-focusing often leads to dramatic intensity amplification with propagation distance. Indeed, self-focusing of light, as described by the nonlinear Schrodinger equation, results in formation of a point singularity after finite distance of light propagation [11, 12]. A finite amount of optical power is drawn into this point, usually referred to as beam collapse. Near singularity, the nonlinear Schrodinger equation loses its applicability because of finite density depletion effects and instead of singularity, light scatters in a wide range of angles, causing loss of precise irradiation symmetry necessary for fusion. For application to fusion, only the 3D regime is relevant, and only this regime is considered in this paper. Note that in some regimes other, high frequency instabilities, such as stimulated Raman scatter can also arrest catastrophic collapse (see e.g. [13]) but they are not considered here.

Beam collapse occurs if the laser beam power, P, exceeds a critical value [12], $P_c \propto T_e/n_e$. T_e and n_e are the electron temperature and density, respectively. For NIF parameters ($n_e \approx 10^{21}\, cm^{-3}$, $T_e \approx 5\,\mathrm{keV}$, $\omega_0 \approx 5 \times 10^{15}\,\mathrm{s}^{-1}$) $P_c = 1.5 \times 10^9\,\mathrm{W}$. This power evaluation

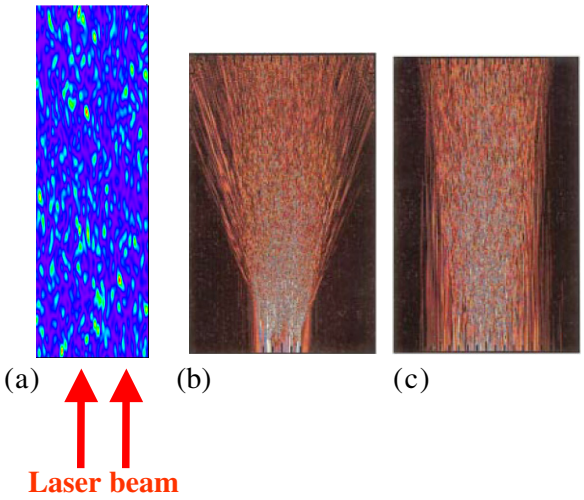

Figure 1. Two dimensional slice of light intensity fluctuations inside plasma. The laser beam propagates from the bottom of the figure upwards. (*a*) Distribution of fluctuations at a scale much smaller than the beam diameter. Random fluctuations ('speckles') are highly anisotropic, with correlation or speckle length along the beam propagation, 'z', direction about $7F^2\lambda_0$. (*b*) Beam spray regime of laser propagation. Beam disintegrates into many small beams. (*c*) Negligible beam spray regime. This regime is necessary for attaining fusion (from [2] with permission). The horizontal scale in (*b*) and (*c*) corresponds to beam diameter.

is based on [12], in contrast to threshold given by Max [14], which is roughly half as large. The former may be dynamically realized (see equation (107) of [15]) from non equilibrium initial conditions, appropriate to initiation by hot spots, while the latter is strictly an equilibrium property and hence not useful for quantitative beam propagation prediction.

The energy required for ICF is so large that the power in each of NIF's 48 beam quads [4] exceeds P_c by several orders of magnitude: the power of each NIF beam is approximately 8×10^{12} W or about 5×10^3 critical power. This difficulty is alleviated by the random phase plate (RPP) [16] which splits the laser beam into many (tens of thousands) small beams with random phases, which are then optically focused into plasma (see figure 2 [2]). As a result the total laser beam electric field amplitude, E, is well approximated in vacuum as an anisotropic random Gaussian field, with correlation length l_c perpendicular to the beam propagation direction, much smaller than the parallel correlation length. The laser intensity, $I \propto |E|^2$, forms a speckle field—a random in space distribution of intensity (see figure 1 (*a*)).

3. Time-independent self-focusing

First consider the regime where laser beam time dependence is negligible. If the average intensity, $\langle I \rangle$, is small, then collapse events occur only in speckles (also referred to as hot spots) with $I \gg \langle I \rangle$, so that their power, $P \sim l_c^2 I$, exceeds P_c. The width of these intense speckles, $F\lambda_0$, is much smaller than the beam diameter and is determined by the laser optic system, where λ_0 is the laser wavelength in vacuum and F is the optic f-number (the ratio of the focal length of the lens divided by the lens diameter). We take $l_c = F\lambda_0/\pi$. Since there is always finite probability of obtaining such collapsing speckles in the random Gaussian field model, the beam angular divergence, $\Delta\theta$, increases with each collapse event. $\Delta\theta$ in vacuum is given by $\Delta\theta = 1/F$, for $F^2 \gg 1$. If the probability of speckle collapse is small, then the beam

will keep its initial form. But if laser power is so large that power of many hot spots exceeds P_c then the beam will disintegrate into many small beams, leading to rapid change in $\Delta\theta$, (beam spray). Figures 1(*b*) and (*c*) show examples of both regimes of strong and negligible beam spray.

An important measure of beam spray in this time-independent regime is the fraction, $P_{\rm scattered}$, of beam power, $P_{\rm beam}$, in speckles which self-focus as the beam propagates, estimated as follows. NIF optic is approximately square, and hence a speckle area is $F^2\lambda_0^2$, implying a critical intensity for speckle self-focusing, $I_c = P_c/(F\lambda_0)^2 \approx 1.9 \times 10^{16}\,\mathrm{W\,cm^{-2}}$.

The *a priori* probability distribution of speckle intensities implies that the mean number M of speckles (local maxima) in volume V with intensities above value I is given by (see equation (21) of [17])

$$M(I) = \frac{\pi^{3/2}\sqrt{5}V}{27F^4\lambda_0^3\pi}\left[\left(\frac{I}{\langle I\rangle}\right)^{3/2} - \frac{3}{10}\left(\frac{I}{\langle I\rangle}\right)^{1/2}\right]\exp\left(-\frac{I}{\langle I\rangle}\right), \tag{1}$$

where $\langle I\rangle = P_{\rm beam}/S$ is the average beam intensity and S is the beam cross section. Then $M(I_c)$ is the number of collapses per volume V and $P_{\rm scattered} = P_c M(I_c)$ is the optical power scattered out of the main beam due to self-focusing. Therefore, rate of scattering is given by

$$P_{\rm beam}^{-1}\,\mathrm{d}P_{\rm scattered}/\mathrm{d}z = \frac{P_c M(I_c)}{\langle I\rangle V}. \tag{2}$$

For NIF parameters, equations (1) and (2) give $P_{\rm beam}^{-1}\,\mathrm{d}P_{\rm scattered}/\mathrm{d}z = 0.0005\,\mathrm{cm^{-1}}$ for $\langle I\rangle = 10^{15}\mathrm{W\,cm^{-2}}$ and $P_{\rm beam}^{-1}\,\mathrm{d}P_{\rm scattered}/\mathrm{d}z = 1.2\,\mathrm{cm^{-1}}$ for $\langle I\rangle = 2\times10^{15}\,\mathrm{W\,cm^{-2}}$. If Max's lower value of P_c were used, order unity of the total beam power would have been predicted to scatter over a typical NIF plasma length of 1 cm, even at the lower intensity since $\mathrm{d}P_{\rm scattered}/\mathrm{d}z$ is exponentially sensitive (see equation (1)) to the parameter α, with $\mathrm{d}P_{\rm scattered}/\mathrm{d}z \propto \exp(-\alpha)$, and $\alpha = I_c/\langle I\rangle$. For NIF parameters, $\alpha \gg 1$.

4. Time-dependent self-focusing

Clearly beam spray due to speckle self-focusing could be a problem at the higher intensity. This is alleviated by temporal beam smoothing techniques [18,19] which induce finite speckle coherence time, T_c: the intensity distribution of light intensity inside plasma is given by a speckle field at each moment of time as in figure 1(*a*) but the location of hot spots changes in a random manner with a typical time T_c. Such techniques are used in contemporary experiments [8] and in future experiments at NIF.

Inertia weakens the plasma density response: if T_c is less than the duration of a particular self-focusing event, $\approx F\lambda_0/c_s\sqrt{P/P_c}$, (this estimate is accurate for $P/P_c \gtrsim 2.5$, see [15]) then this self-focusing event will be suppressed. This suppression effect is significant if $T_c \lesssim F\lambda_0/c_s$, i.e. T_c must be smaller than the time it takes for a sound wave to cross a speckle width ($\sim$4 ps for NIF parameters). Here c_s is the ion-acoustic wave speed. (This is in contrast to the case of almost instantaneous response of optical Kerr nonlinearity which is typical for solids [5].) As T_c decreases, a smaller fraction of the beam power participates in collapse events, controlled by the parameter $\propto\alpha(l_c/c_sT_c)^2$, instead of α, for time-independent self-focusing. This has led to the common assumption [4] that if the total power participating in independent collapse events is made arbitrarily small by reducing T_c, then beam spray could be reduced to any desired level.

However, we have found [7] that even for very small T_c, self-focusing can lead to strong beam spray. Now, self-focusing results from a collective instability, CFSBS, which couples the beam to ion acoustic waves that propagate transversely to the direction of laser

beam propagation. As l_c increases, the well-known dispersion relation of forward stimulated Brillouin scattering [20] is recovered for coherent laser beam. We predict that this instability is not a sensitive function of T_c for $c_s T_c \lesssim F\lambda_0$. Recent experiments at the Omega laser facility [8] are in excellent agreement with that prediction: it was found that reducing T_c from 3.4 ps (for which $c_s T_c \approx F\lambda_0$) to 1.7 ps did not cause a further reduction of beam spray at $\langle I \rangle = 5 \times 10^{14}\,\mathrm{W\,cm^{-2}}$. Note that the dominant seed for CFSBS is not thermal but time-dependent plasma density fluctuations caused by fluctuating speckles.

5. Thermal self-focusing

Quantitative comparison with this data requires an extension of our earlier work [7] to include fluctuations in electron temperature, δT_e. In that case thermal self-focusing comes into play. Propagation of the laser beam envelope at electron densities, n_e, small compared with critical, n_c, is described by the paraxial equation for the electric field spatiotemporal envelope, E,

$$\left(i\frac{\partial}{\partial z} + \frac{1}{2k_0}\nabla^2 - \frac{k_0}{2}\frac{n_e}{n_c}\rho\right)E = 0, \qquad \nabla = \left(\frac{\partial}{\partial x}, \frac{\partial}{\partial y}\right), \tag{3}$$

which is coupled to the linearized hydrodynamic equation for the relative density fluctuation, $\rho = \delta n_e / n_e$, as it propagates acoustically with acoustic speed c_s:

$$\left(\frac{\partial^2}{\partial t^2} + 2\tilde{\nu}\frac{\partial}{\partial t} - c_s^2\nabla^2\right)\ln(1+\rho) = c_s^2\nabla^2\left(I + \frac{\delta T_e}{T_e}\right), \tag{4}$$

where $k_0 = 2\pi/\lambda_0$, $I = |E|^2$ is the light intensity and $\tilde{\nu}$ is an integral operator whose Fourier transform in x and y is $\nu_{ia} k c_s$, where ν_{ia} is the ion acoustic wave amplitude damping rate normalized to the ion acoustic frequency. x and y are transverse directions to beam propagation direction z. E is in thermal units defined so that in equilibrium, with uniform E, the standard $\rho = \exp(-I) - 1$ is recovered. $n_c = m_e\omega_0^2/4\pi e^2$ is the critical electron density, m_e is the electron mass and e is the electron charge. The relative electron temperature fluctuation, $\delta T_e / T_e$, is responsible for thermal self-focusing and was omitted in our previous work [7].

We make the ansatz that the Fourier transform of electron temperature fluctuation, $\delta T_e(k)/T_e$, satisfies

$$\left(\tau_{ib}\frac{\partial}{\partial t} + 1\right)\frac{\delta T_e(k)}{T_e} = g(k\lambda_e)I(k), \tag{5}$$

which is a reduced version of Epperlein's model [25]. Here the right-hand-side (r.h.s.) determines plasma heating by the inverse bremsstrahlung, $I(k)$ is the Fourier transform of I, so that intensity fluctuations are a source of δT_e [9]. The inverse bremsstrahlung relaxation time, τ_{ib}, is given by

$$\tau_{ib} = \frac{1}{kc_s}\frac{3}{128}\sqrt{\frac{\pi Z^*\phi}{2}}\frac{\left[1 + (30k\lambda_e)^{4/3}\right]}{k\lambda_e}\frac{c_s}{v_e}. \tag{6}$$

Also

$$g(k\lambda_e) = \frac{\left[1 + (30k\lambda_e)^{4/3}\right]}{96(k\lambda_e)^2}Z^*, \tag{7}$$

and ϕ is an empirical factor [23], $\phi = (4.2 + Z^*)/(0.24 + Z^*)$, $Z^* = \sum_i n_i Z_i^2 / \sum_i n_i Z_i$ is the effective plasma ionization number and n_i and Z_i are the number density and the ionization number (number of ionized electrons per atom) of ith ion species of plasma, respectively. λ_e is related to the standard e–i mean free path, λ_{ei}, by

$$\lambda_e = (\lambda_{ei}/3)(2Z^*/\pi\phi)^{1/2}. \tag{8}$$

The basic ion acoustic wave parameters, $\nu_{\rm ia}$ and $c_{\rm s}$, are regarded as given by kinetic theory [27–29] which, for example, takes into account the effect of compressional heating on sound wave propagation. For comparison with the experiment in this paper, however, collisionless theory is used for the evaluation of acoustic wave parameters.

Equation (5) implies that thermal conductivity is determined by

$$\kappa = \frac{3}{2}\frac{n_{\rm e}}{\tau_{\rm ib}k^2} = \frac{\kappa_{\rm SH}}{1+(30k\lambda_{\rm e})^{4/3}}, \tag{9}$$

where $k_{\rm SH}$ is the classical Spitzer–Harm [21] thermal conductivity coefficient in plasma. Since $l_{\rm c}$ is *not* large compared with the electron ion mean free path, $\lambda_{\rm ei}$, thermal transport becomes nonlocal, and $\kappa_{\rm SH}$ is effectively reduced, as given by equation (9), when applied to a fluctuation at speckle wavenumbers, $k = O(1/l_{\rm c})$. This reduction of $\kappa_{\rm SH}$ is substantial for the experiment of [8], implying much larger $\delta T_{\rm e}$ than classical transport [25]. The importance of the thermal contribution to self-focusing at the speckle scale was first realized by Epperlein [22, 25], on the basis of Fokker–Planck simulations, and later analytically derived [24] and verified experimentally [26]. It was recently realized [27,28] that Epperlein's result [22,25] is correct provided the acoustic frequency, $c_{\rm s}/l_{\rm c}$, is smaller than the electron–ion collision frequency, $v_{\rm e}/\lambda_{\rm ei}$. Also see [30,31] for more discussion.

To solve equations (3),(4) and (5) we need to determine boundary conditions on E. We assume, absent plasma, that in the optic far field the Fourier spectrum of E is top-hat with square shape:

$$|\hat{E}(\mathbf{k})| = \text{const for } |k_x| < k_m \text{ and } |k_y| < k_m; \qquad |\hat{E}(\mathbf{k})| = 0, \text{ otherwise}, \tag{10}$$

where $k_m = l_{\rm c}^{-1}$ and $\mathbf{k} = (k_x, k_y)$ is the transverse (to the laser beam) wavevector. The superposition of all these Fourier modes propagating in uniform density plasma we refer to as E_0, the solution of equation (3) with $\rho = 0$. We assume temporal beam smoothing which means that Fourier modes $\hat{E}(\mathbf{k})$ with different $\mathbf{k}$ are uncorrelated and the modes with the same $\mathbf{k}$ are correlated with short correlation time $T_{\rm c} < l_{\rm c}/c_{\rm s}$.

For NIF designs, Z^* is highly variable depending on details of plasma composition. Laser beam may pass through, for example, He, Be, CH, SiO_2 and Au plasma, allowing a wide range of Z^*. When Z^* is small, thermal effects are small, and our previous ponderomotive theory [7] applies. In this case, the linear stage of the collective instability depends only on one parameter—dimensionless intensity [7],

$$\tilde{I}_0 = \frac{4F^2}{\nu_{\rm ia}}\frac{n_{\rm e}}{n_{\rm c}}I_0 \propto \frac{1}{\alpha\nu_{\rm ia}}. \tag{11}$$

I_0 is the spatial average of $|E|^2$. Note that the standard figure of merit for self-focusing, $1/\alpha$, is smaller by the factor $\nu_{\rm ia}$ (see [4]).

6. Collective forward stimulated Brillouin scatter and transition to beam spray regime

For small $T_{\rm c}$, one might expect $\rho \simeq 0$ and that the laser beam would propagate with $E = E_0$. However, linearization of equations (3), (4) and (5) in E and ρ about this state shows that this propagation is unstable. Following the ideas of [7] and setting $\rho = \delta\rho e^{\lambda z}\exp[i(\mathbf{k}\cdot\mathbf{x} - \omega t)]$, $E = E_0 + \delta E e^{\lambda z}\exp[i(\mathbf{k}\cdot\mathbf{x} - \omega t)]$, we obtain the following dispersion relation, at acoustic resonance $\omega = kc_{\rm s}$, assuming $\mathbf{k}$ parallel to either the x or y directions:

$$2i\nu_{\rm ia} = \left[1 + \frac{g(k\lambda_{\rm e})}{1 - ikc_{\rm s}\tau_{\rm ib}}\right]\frac{\delta I}{\delta\rho}, \tag{12}$$

where the plasma density response function $\delta I/\delta\rho$ is given by

$$\frac{\delta I}{\delta\rho} = \frac{n_e}{n_c}\frac{k_0^2 I_0}{4kk_m}\ln\frac{k^2(-2k_m+k)^2+4k_0^2\lambda^2}{k^2(2k_m+k)^2+4k_0^2\lambda^2}. \tag{13}$$

In the general case of the arbitrary direction of **k** the dispersion relation is much more bulky and not given here because it gives essentially the same result. One finds a range $0 < k < k_{\text{cutoff}}$ of unstable modes ($Re(\lambda) > 0$).

One must exercise caution in using equations (12) and (13) since they ignore density fluctuations which are enhanced above thermal level by laser beam intensity fluctuations. In general these fluctuations are always important as an instability seed. However, as T_c decreases, their magnitude and effect on beam divergence decrease once T_c is smaller than the slow hydrodynamic time scale, $1/k_m c_s$. As a measure of beam angular divergence we take

$$\Delta\langle\Theta^2\rangle(z) = \langle\Theta^2\rangle(z) - \langle\Theta^2\rangle(0), \tag{14}$$

where

$$\langle\Theta^2\rangle = k_0^{-2}\int k^2|\hat{E}(\mathbf{k})|^2 d\mathbf{k}/\int|\hat{E}(\mathbf{k})|^2 d\mathbf{k}. \tag{15}$$

If the beam angular diffusion rate $D \equiv (d/dz)\langle\Theta^2\rangle$ due to these fluctuations is small compared with the instability growth rate as given by equation (12), $D \ll \lambda_{\max}$, then the dispersion relation (12) is accurate [7]. In dimensionless units

$$\tilde{D} \ll \tilde{\lambda}_{\max}. \tag{16}$$

Here $\tilde{D}$ is the dimensionless diffusion coefficient for beam angular divergence $\tilde{D} = (16F^4/k_0)D$ and $\tilde{\lambda}_{\max}$ is the maximum value of $Re(\tilde{\lambda})$ which is achieved at $k = k_{\max}$, where $\tilde{\lambda} \equiv l_c^2 k_0 \lambda$ is the dimensionless growth rate. In other words, T_c does not enter the dispersion relation if T_c is small enough so that equation (16) is satisfied.

It was shown in [7] for the pondermotive case that

$$\tilde{D} \approx \nu_{ia}\tilde{T}_c\tilde{I}_0^2/100, \tag{17}$$

where $\tilde{T}_c \equiv k_m c_s T_c$ is the dimensionless coherence time. Thermal effects increase the level of density fluctuations changing the condition (16) qualitatively through the replacement of $\tilde{I}_0$ by $[1 + g(k_m\lambda_e)]\tilde{I}_0$. Equations (16) and (17) determine the domain of validity of dispersion relation (12). We illustrate the use of the condition (16) in several examples below.

In addition to the scattering from the enhanced density fluctuations, the collapse of intense speckles also contributes to beam divergence as was discussed in section 3. One such process is the resonant filament instability [32] which requires speckles with power of at least $3P_c$. The estimate of the importance of resonant instability in beam divergence may be obtained by comparing the CFSBS instability growth rate $\lambda_{\max}$ with the rate determined by equation (2) with I_c replaced by $3I_c$:

$$P_{\text{beam}}^{-1} dP_{\text{scattered}}/dz \ll \lambda_{\max}. \tag{18}$$

For time-independent self-focusing, $P_{\text{beam}}^{-1} dP_{\text{scattered}}/dz \propto \exp(-3\alpha)$. For time-dependent self-focusing, (finite speckle coherence time T_c) α is reduced by a factor $\propto\alpha(l_c/c_s T_c)^2$ (see section 4). Inequality (18) is very well satisfied for both NIF parameters and parameters of experiment [8]. For NIF parameters with $I = 2\times10^{15}\,\text{W cm}^{-2}$ we obtain that $\alpha \approx 9.6$ and $P_{\text{beam}}^{-1} dP_{\text{scattered}}/dz \approx 9\times10^{-8}\text{cm}^{-1}$ and therefore is irrelevant compared with CFSBS. For beam spray onset intensity $I = 1.5\times10^{14}\,\text{W cm}^{-2}$ of experiment [8] we find that $\alpha \approx 12$ and therefore resonant instability is also irrelevant. However for the largest intensity of that experiment, $I = 10^{15}\,\text{W cm}^{-2}$, we find that $\alpha \approx 1.8$ which implies that absent finite T_c effects

$P_{\rm beam}^{-1}{\rm d}P_{\rm scattered}/{\rm d}z \approx 20\,{\rm cm}^{-1}$. This is an overestimate because finite $T_{\rm c}$ enhancement of α is neglected here. Thus the dispersion relation (12) is clearly relevant for the prediction of the beam spray onset in experiment [8], but the resonant filament instability may be significant for the highest intensity considered in this experiment.

Note that for $k_m \to 0$ ($F^2 \gg 1$) equation (13) reduces to

$$\frac{\delta I}{\delta \rho} = -\frac{n_{\rm e}}{n_{\rm c}} \frac{2k^2 k_0^2 I_0}{4k_0^2\lambda^2 + k^4}, \tag{19}$$

which means that equation (12), absent thermal effects (i.e. for $\delta T_{\rm e} = 0$ in equation (4)), reduces to the paraxial limit of the standard FSBS dispersion relation [20].

With absent thermal effects we regain the pondermotive case considered in [7] except that in this paper square top hat boundary conditions (10) are used compared with circular top hat boundary conditions used in [7]. We find however that both circular and square top hat boundary conditions give similar results.

$\tilde{\lambda}_{\rm max}$ only depends on

$$\tilde{I} \equiv \left[1 + \frac{g(k_{\rm max}\lambda_{\rm e})}{1 - ik_{\rm max}c_s\tau_{\rm ib}}\right]\tilde{I}_0. \tag{20}$$

Here $\tilde{I}_0$ is given by (11). According to our theory of CFSBS, $\lambda_{\rm max}^{-1}$ should be compared with the basic correlation length in z direction, known as the speckle length, $l_{\rm speckle} \approx 7F^2\lambda_0$. The value $\tilde{\lambda}_{\rm max} = 0.1$, at which $\lambda^{-1} \approx l_{\rm speckle}$, marks regime transition. At this transition we find that $k_{\rm max} \approx k_m/2$. In the weak regime, with $\tilde{\lambda}_{\rm max} \ll 0.1$, there is little gain over a speckle length. It follows that only small changes in correlations develop over a speckle length, in particular there is little change in $\Delta\langle\Theta^2\rangle$. Changes over different speckles are uncorrelated, leading to a quasi-equilibrium (see figure 3 of [7]). As $\tilde{\lambda}$ crosses the value 0.1 (corresponding to $\tilde{I} \approx 2$ in ponderomotive case), the non equilibrium regime is entered and beam properties change rapidly with z. In particular, $\Delta\langle\Theta^2\rangle$ changes rapidly, i.e. there is a strong beam spray. This is shown in figure 2, where normalized beam angular divergence $\propto\Delta\langle\Theta^2\rangle/\tilde{I}_0^2$ is shown from direct simulations for parameters $n_{\rm e}/n_{\rm c} = 0.1$, $T_{\rm e} = 5\,{\rm keV}$, $\omega_0 = 5.37 \times 10^{15}\,{\rm s}^{-1}$, $c_{\rm s} = v_{\rm e}/60$, $F = 8$, $\nu_{\rm ia} = 0.0375$, $\tilde{T}_{\rm c} = 1/8$ and plasma length $z_{\rm length} = 15.7k_0/k_m^2$ (i.e. $z_{\rm length} \approx 1.3l_{\rm speckle}$). This normalization is natural because the diffusion coefficient $\tilde{D}$ varies as $\tilde{I}_0^2$ (see equation (17) and also see [7] for more discussion). Variation of $\tilde{I}_0$ in simulations of figure 2 is achieved solely by variation of laser intensity. The rapid departure of both curves of figure 2(*b*) from the horizontal line with increase in $\tilde{I}_0$ is a result of CFSBS instability.

Typically, in real experiments, $\tilde{T}_{\rm c}$ is closer to 1 than 1/8. If in simulations $\tilde{T}_{\rm c} = 1$ is used instead of 1/8, then the instability seed amplitude would be $\sqrt{8}$ larger with the result that for the larger values of $\tilde{I}_0$ it would be more difficult to distinguish between linear and nonlinear effects. But even if $\tilde{T}_{\rm c} = 1$ and for the largest laser intensity, the dispersion relation (12) is valid. In the strongest pondermotive case (see black curves in figure 2) we have $\tilde{I}_0 = 3.8$ ($\tilde{\lambda} = 0.3$) so that equations (16) and (17) imply $\tilde{T}_{\rm c}\tilde{I}_0^2 \ll 800$ which is very well satisfied. In the strongest thermal case ($g(k_m\lambda_{\rm e}) = 1.3$, $\tilde{I}_0 = 1.9$, $\tilde{\lambda} = 0.3$, see red curves in figure 2) the condition (16) is again very well satisfied.

Figures 2(*a*) and (*b*) differ by the important change of independent variable from $\tilde{\lambda}$ to $\tilde{I}$, which allows a unified presentation of both ponderomotive and thermal cases. In the linear regime one expects that the growth rate λ provides a complete description of the system. For example, for $Re(\tilde{\lambda}) \ll 0.1$ the two curves of figure 2(*b*), which are quite different, collapse to the same curve in figure 2(*a*) as expected in a linear regime. Surprisingly, even for large values of $Re(\tilde{\lambda})$, e.g. $Re(\tilde{\lambda}) = 0.3$, which shows strong saturation effects as seen in figure 2(*a*), the curves again collapse.

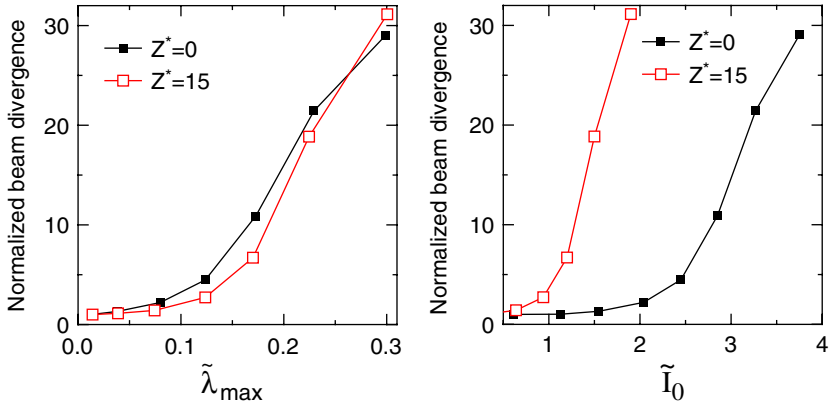

Figure 2. Normalized beam angular divergence obtained from nonlinear simulation with NIF parameters as a function of (*a*) dimensionless growth rate $\tilde{\lambda}$ and (*b*) dimensionless intensity $\tilde{I}$. Black curves (■) correspond to ponderomotive self-focusing ($Z^* = 0$) and red curves (□, $Z^* = 15$) correspond to the case where both ponderomotive and thermal self-focusing are essential. Both red and black curves collapse to the single curve in (*a*) which indicates that $\tilde{\lambda}$ is a much better parameter for the onset of beam spray, compared with $\tilde{I}$. For example, $\tilde{I}_0 = 1.9$ corresponds to intensity $I = 1.3 \times 10^{15}\,\mathrm{W\,cm^{-2}}$ in physical units. In this figure, for each curve, beam angular divergence is normalized to unity at the lowest intensity shown.

As a guide to the validity of the paraxial wave approximation we present here the analytical results for k_{cutoff} and k_{max}, applicable, in particular, to the cases shown in figure 2. In the pondermotive regime (replace brackets in equation (20) by 1 which corresponds to formally setting $Z^* = 0$) we find

$$\tilde{k}_{\mathrm{cutoff}} \approx \frac{\pi \tilde{I}_0}{8}. \tag{21}$$

In the thermally dominated regime, when the second term in the brackets of equation (20) is larger than 1 and $kc_s\tau_{\mathrm{ib}} < 1$, we obtain

$$\tilde{k}_{\mathrm{cutoff}} \simeq \left(\frac{\pi \tilde{I}_0}{768} 30^{4/3} (k_m \lambda_e)^{-2/3} Z^*\right)^{3/5}. \tag{22}$$

We find from numerical solution of dispersion relation (12) that in both cases corresponding to equations (21) and (22) $k_{\mathrm{max}} \approx k_{\mathrm{cutoff}}/2$ (with accuracy of about 20%).

Specifically for the most strongly unstable case of red curve of figure 2 with $\tilde{I}_0 = 1.9$ we find that according to equation (22) $k_{\mathrm{cutoff}} \approx k_0/2F$. Note for that particular set of parameters pondermotive effects are also significant so that the solution of equation (12) gives $k_{\mathrm{cutoff}} \approx 1.4k_0/2F$. Therefore, if the paraxial wave approximation is initially valid, $F^2 \gg 1$, it remains so as the beam propagates through plasma because $k^2_{\mathrm{cuttoff}} \ll k_0^2$. This guide is based on the linear theory and is valid provided nonlinear effects are small. Nonlinear simulation for the strongest case ($\tilde{I}_0 = 1.9,\ Z^* = 15$) shows that the beam angular divergence increases by a factor of about 2; in other words, the beam speckle length decreases by a factor 4 so that paraxial wave approximation remains valid.

The identification of $\tilde{\lambda}_{\mathrm{max}} = 0.1$ as the transition between weak and strong beam spray regimes leads to a practical algorithm for evaluating the laser intensity at this transition. In our study of the validity of paraxial wave approximation we find that $\tilde{k}_{\mathrm{max}} \approx 1/2$ and $Im(\tilde{\lambda}) \approx 1/2$ at CFSBS regime transition, $\tilde{\lambda}_{\mathrm{max}} = 0.1$. This provides a simple expression for the laser intensity at regime transition as follows: substitute in equations (12) and (13) $k = k_m/2$ and

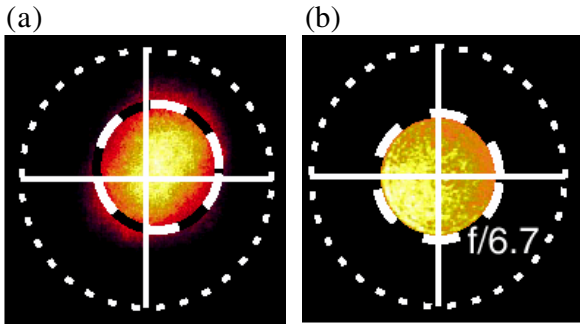

Figure 3. Experimental images of the cross section of time averaged laser beam intensity after propagation through plasma. (*a*) Onset of beam spray regime at $5 \times 10^{14}\,\mathrm{W\,cm^{-2}}$. (*b*) Negligible beam spray regime achieved by lowering intensity. The dashed circles correspond to $F = 6.7$ beam width for propagation in vacuum. Reproduced from [8] with permission.

$\lambda = (0.1 + i\,0.5)k_m^2/k_0$. Recall that $k_m = k_0/(2F)$. λ_e, g and τ_{ib} are given by equations (8),(7) and (6), respectively. The resulting linear expression for I_0 will have real and imaginary parts because an approximate value for $\lambda = (0.1 + i\,0.5)k_m^2/k_0$ is used. Ignore the imaginary part to obtain an explicit expression for the laser intensity at beam spray onset:

$$I_{0,\mathrm{beamspray}} = \frac{\nu_{ia}}{4F^2}\frac{n_c}{n_e} Re\left[(2.2 - i\,0.31)\left(1 + \frac{g(k_m\lambda_e/2)}{1 - ik_m c_s \tau_{ib}/2}\right)^{-1}\right]. \tag{23}$$

We find that both for NIF parameters and parameters of experiment [8], the error in the real part of I_0 is less than 20% for $Z^* < 20$. Recall we use here thermal units, so that the laser intensity $I_0 = (1/4)(v_{osc}/v_e)^2$, where v_{osc} is the quiver velocity of the electron in the laser's electromagnetic field. We suggest equation (23) as a simple guide for the onset of beam spray. If necessary equation (23) may be compared with the numerical solution of dispersion relation (12).

Thus analysis of $\tilde{\lambda}$ results in the second and main conclusion of our CFSBS theory: prediction of the onset of beam spray, and hence a prediction of the fundamental limit on power propagation. Here we present a comparison of this prediction with [8], the first experimental measurement of beam spray onset (see figure 3). From [8, 33, 34][5,6] we find that $0.14 < n_e/n_c < 0.25$. $T_e \sim 2\,\mathrm{keV}$, $F = 6.7$ $\omega_0 \approx 3.6 \times 10^{15}\,\mathrm{s^{-1}}$ and $Z^* = 6.4$ at the upper range of densities. For a nominal electron density of $n_e = 0.2n_c$, the 0.1 contour of $\tilde{\lambda}$ is shown in figure 4(*a*), implying $\tilde{I} \approx 0.66$ at regime transition. The lowest intensity, $1.5 \times 10^{14}\,\mathrm{W\,cm^{-2}}$, at which scatter was observed [8], corresponds to $\tilde{I}_0 \approx 1.05$, with Landau damping $\nu_{ia} = 0.06$ for the plasma composition at this density. The major uncertainty in comparing this data with theory is due to the significant time dependence of T_e/T_i (which implies uncertainty in ν_{ia}) during experiments as well as plasma density inhomogeneity, e.g. if $n_e = 0.14n_c$ (which corresponds to plasma density plateau in figure 3 of [8]) with other parameters the same, then theory predicts $\tilde{I}_0 \approx 0.73$ and experiments give $\tilde{I}_0 \approx 0.82$. In contrast, prediction based on speckle collapse, with critical power P_c, gives that even at the maximum density of $n_e/n_c = 0.25$ $P_{\mathrm{beam}}^{-1}\mathrm{d}P_{\mathrm{scattered}}/\mathrm{d}z = 0.23\,\mathrm{cm^{-1}}$, the scattered power fraction, $P_{\mathrm{scattered}}/P_{\mathrm{beam}}$, is only 0.5% after 200 μm of propagation through the high-density region of the plasma. This is much less than the observed [8] 10%. Therefore, beam spray due to CFSBS is consistent with the data while beam spray due to speckle collapse is not.

[5] We thank C Niemann for communicating to us the detailed plasma composition.
[6] Determined by simulation, results provided by N B Meezan [34].

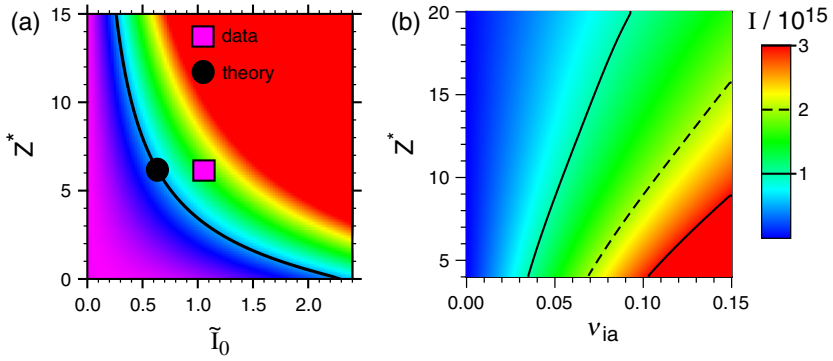

Figure 4. (*a*) Solid curve separates predicted beam spray regime, $\tilde{\lambda} > 0.1$ (from green to red colours, i.e. from curve centre to upper right hand corner), from negligible beam spray regime $\tilde{\lambda} < 0.1$ (from blue to purple colours, i.e. from curve centre to lower left hand corner). Different colours denote values of $\tilde{\lambda}$, with red corresponding to the value 0.3 and above. The magenta square denotes experimentally measured ([8]) beam spray onset, assuming $\nu_{ia} = 0.06$ and the black circle is the theoretical prediction for $\nu_{ia} = 0.06$. (*b*) Predicted onset of beam spray regime (i.e. for $\tilde{\lambda} = 0.1$) as a function of Z^* and ν_{ia} for the NIF plasma with $T_e \sim 5\,\mathrm{keV}$, $F = 8$, $n_e/n_c = 0.1$, $\omega_0 \approx 5.4 \times 10^{15}\,\mathrm{s}^{-1}$. Colours show laser intensity, in units of $10^{15}\,\mathrm{W\,cm}^{-2}$, with the (solid) contour curve in the lower right hand corner corresponding to an intensity of $3 \times 10^{15}\,\mathrm{W\,cm}^{-2}$. Intensity is at maximum for small Z^* and large ν_{ia}. We assume $Z^* > 4$ to make sure that condition $c_s/l_c < \nu_e/\lambda_{ei}$ is true.

7. Implication for backscattering

Recent experiments at the Atomic Weapon Establishment in the UK have demonstrated a reduction of both stimulated Brillouin and Raman backscatter [35] by the addition of small amounts of high ionization state dopants to a low ionization state plasma, e.g. a 1% dopant reduced backscatter by more than an order of magnitude. The combination of these experimental facts with our prediction that dopant may cause transition to beam spray regime suggests that one should expect anti-correlation between beam spray and backscatter. If this anti-correlation is confirmed experimentally then we propose the following mechanism: beam spray decreases speckle length (correlation length) with beam propagation and backscatter is suppressed by the reduction of the laser beam correlation length. The latter has been established through simulation [13], experiment [36] and one-dimensional analytic theory [37]. In other words, the control of backscatter is achieved indirectly through control of CFSBS. We are unaware of any other explanation of this backscatter reduction by the addition of small amounts of high Z dopant [38][7].

Clearly, to maintain control of forward beam propagation, beam spray must not be strong. If plasma paramters are conducive to backscatter as in the Atomic Weapon Establishment experiment [35], then by altering the plasma state so as to be above, but close to, the beam spray regime transition, allowing moderate beam spray might lead to optimum control of beam propagation and backscatter. This suggests operating above but, for example, close to the solid curve of figure 4(*a*) which marks the transition regime of CFSBS.

[7] After submitting this paper we found from discussion with J Kline [38] that another possible explanation is the increase of absorption of backscatter due to the increase of bremsstrahlung with high Z dopant.

8. Conclusion

In conclusion, transition to the beam spray regime was recognized as a collective phenomenon [39][8]. Our theory is in excellent agreement with experiment: the transition laser intensity and its insensitivity to changes in correlation time were predicted. We found that the growth rate of CFSBS depends on four dimensionless parameters: the scaled laser intensity $\tilde{I}_0$ (see equation (11)), scaled electron–ion mean free path $\lambda_{ei}/F\lambda_0$, effective ionization number Z^* and c_s/v_e. The first three of these can be manipulated experimentally. So our theory permits predictions for beam control at the NIF that may be implemented since thermal self-focusing can be manipulated experimentally through the control of CFSBS in two ways. First, by changing Z^* through change of plasma composition. For example, the addition of 1% of Xenon (high Z dopant) to low Z plasma (50% of He and 50% of H) would increase Z^* from 1.7 to 15.5 without a significant change in ν_{ia}. Second, beam control can be implemented by adding low Z dopant to a high Z plasma, e.g. adding He to $Si0_2$, in order to increase ν_{ia} at almost constant Z^*. Figure 4(*b*) shows the dependence of laser intensity (indicated by colours) at predicted onset of beam spray regime on Z^* and ν_{ia} for NIF parameters. It is seen that maximal allowable intensity occurs for small Z^* and large ν_{ia}. We propose figure 4(*b*) as a direct guide for the choice of NIF designs to attain maximum power of laser beam, which may propagate without significant beam spray.

The observation of anti-correlation between beam spray and backscatter, through the addition of small amounts of high Z dopant, would mean additional confirmation of our theory. We predict that the control of backscatter is achieved indirectly through the control of CFSBS, e.g. by changing plasma ionization state and/or acoustic damping [40][9].

Acknowledgments

The authors thank R L Berger for drawing our attention to [27, 28] and pointing out that the seed for CFSBS provided by the fluctuating speckles is much larger than the thermal. The authors also thank W Rozmus for pointing out the limitation of Epperlein's model [22, 25] to $c_s/l_c < v_e/\lambda_{ei}$. Support was provided by the Department of Energy, under contract DE-AC52-06NA25396.

References

[1] McCrory R L *et al* 1988 *Nature* **335** 225
[2] Still C H *et al* 2000 *Phys. Plasmas* **7** 2023
[3] Miller G H, Moses E I and Wuest C R 2004 *Nucl. Fusion* **44** S228
[4] Lindl J D *et al* 2004 *Phys. Plasmas* **11** 339
[5] Boyd R W 2002 *Nonlinear Optics* (San Diego: Academic)
[6] Sulem C and Sulem P L 1999 *Nonlinear Schroedinger Equations: Self-Focusing and Wave Collapse* (Berlin: Springer)
[7] Lushnikov P M and Rose H A 2004 *Phys. Rev. Lett.* **92** 255003
[8] Niemann C *et al* 2005 *Phys. Rev. Lett.* **94** 085005
[9] Kruer W L 1990 *The Physics of Laser Plasma Interactions* (New York: Addison-Wesley)
[10] Zakharov V E and Shabat A B 1971 *Zh. Eksp. Teor. Fiz.* **61** 118
Zakharov V E and Shabat A B 1972 *Sov. Phys.—JETP* **34** 62
[11] Chiao R Y, Garmire E and Townes C H 1964 *Phys. Rev. Lett.* **13** 479
[12] Talanov V I 1965 *JETP Lett.* **2** 138
[13] Rose H A and DuBois D F 1994 *Phys. Rev. Lett.* **72** 2883–6

[8] To some extent, similar analysis in a different physical context was discussed by [39].
[9] Reduction of stimulated Raman backscatter by reducing acoustic damping has been observed in [40].

[14] Max C E 1976 *Phys. Fluids* **19** 74
[15] Rose H A and DuBois D 1993 *Phys. Fluids* B **5** 3337
[16] Kato Y and Mima K 1982 *Appl. Phys.* B **29** 186
[17] Garnier J 1999 *Phys. Plasmas* **6** 1601 (equation (21))
[18] Lehmberg R H and Obenschain S P 1983 *Opt. Commun.* **46** 27
[19] Skupsky S *et al* 1989 *J. Appl. Phys.* **66** 3456
[20] Schmitt A J and Afeyan B B 1998 *Phys. Plasmas* **5** 503
[21] Spitzer L Jr and Harm R 1953 *Phys. Rev.* **89** 977
[22] Epperlein E M 1990 *Phys. Rev. Lett.* **65** 2145
[23] Epperlein E M and Short R W 1992 *Phys. Fluids* B **4** 2211
[24] Maximov A V and Silin V P 1993 *Zh. Eksp. Teor. Fiz.* **103** 73
Maximov A V and Silin V P 1993 *Sov. Phys.—JETP* **76** 39
[25] Epperlein E M and Short R W 1994 *Phys. Plasmas* **1** 3003
[26] Montgomery D S, Johnson R P, Rose H A, Cobble J A and Fernandez J C 2000 *Phys. Rev. Lett.* **84** 678
[27] Brantov A V *et al* 2004 *Phys. Rev. Lett.* **93** 125002
[28] Berger R L, Valeo E J and Brunner S 2005 *Phys. Plasmas* **12** 062508
[29] Berger R L, and Valeo E J 2005 *Phys. Plasmas* **12** 032104
[30] Brantov A V, Bychenkov V Yu, Tikhonchuk V T, Rozmus W and Senecha V K 1999 *Phys. Plasmas* **6** 3002
[31] Bychenkov V Yu, Rozmus W, Brantov A V and Tikhonchuk V T 2000 *Phys. Plasmas* **7** 1511
[32] Pesme D, Rozmus W, Tikhonchuk V T, Maximov A, Ourdev I and Still C H 2000 *Phys. Rev. Lett.* **84** 278
[33] Niemann C 2005 private communication
[34] Meezan N B 2005 private communication
[35] Suter L J *et al* 2004 *Phys. Plasmas* **11** 2738
[36] Fernandez J C *et al* 1996 *Phys. Rev.* E **53** 2747
[37] Mounaix Ph 1995 *Phys. Plasmas* **2** 1804
[38] Kline J 2006 private communication
[39] Vedenov A A and Rudakov L I 1965 *Sov. Phys.—Dokl.* **9** 1073
Vedenov A A and Rudakov L I 1964 *Dokl. Akad. Nauk SSR* **159** 767
Rurenchik A M 1976 *Radiophys. Quantum. Electron.* **17** 1249
Zakharov V E, Musher S L and Rubenchik A M 1985 *Phys. Rep.* **129** 285–366
[40] Fernandez J C *et al* 1997 *Phys. Plasmas* **4** 1849